Title
Adenosine Triphosphate and Carbon Efficient Route to Second Generation Biofuel Isopentanol.

Journal
ACS synthetic biology, 9(3)

ISSN
2161-5063

Authors
Eiben, Christopher B
Tian, Tian
Thompson, Mitchell G
et al.

Publication Date
2020-03-01

DOI
10.1021/acssynbio.9b00402

Peer reviewed

ACS SyntheticBiology

pubs.acs.org/synthbio Letter

Adenosine Triphosphate and Carbon Efficient Route to Second Generation Biofuel Isopentanol

Christopher B. Eiben, Tian Tian, Mitchell G. Thompson, Daniel Mendez-Perez, Nurgul Kaplan, Garima Goyal, Jennifer Chiniquy, Nathan J. Hillson, Taek Soon Lee, and Jay D. Keasling*

Cite This: https://dx.doi.org/10.1021/acssynbio.9b00402 Read Online

ACCESS | Metrics & More | Article Recommendations | Supporting Information

ABSTRACT: Climate change necessitates the development of CO_2 neutral or negative routes to chemicals currently produced from fossil carbon. In this paper we demonstrate a pathway from the renewable resource glucose to next generation biofuel isopentanol by pairing the isovaleryl-CoA biosynthesis pathway from *Myxococcus xanthus* and a butyryl-CoA reductase from *Clostridium acetobutylicum*. The best plasmid and *Escherichia coli* strain combination makes 80.50 ± 8.08 (SD) mg/L of isopentanol after 36 h under microaerobic conditions with an oleyl alcohol overlay. In addition, the system also shows a strong preference for isopentanol production over prenol in microaerobic conditions. Finally, the pathway requires zero adenosine triphosphate and can be paired theoretically with nonoxidative glycolysis, the combination being redox balanced from glucose thus avoiding unnecessary carbon loss as CO_2. These pathway properties make the isovaleryl-CoA pathway an attractive isopentanol production route for further optimization.

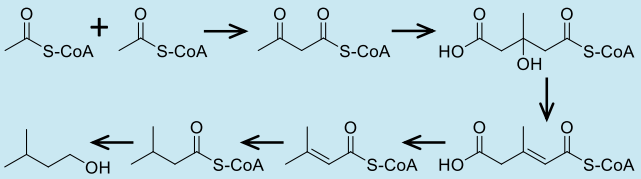

KEYWORDS: *isopentanol, isovaleryl-CoA pathway, biofuel*

Anthropogenic climate change represents a significant challenge for modern society, with transportation activities and petrochemical production contributing about 7 gigatonnes of CO_2 equivalents annually.[1] Sugar-derived biofuels and bioproducts offer an alternate source of these necessary molecules at lower CO_2 emissions.[2] First generation biofuels, ethanol and biodiesel, have drawbacks compared to fossil fuels in internal combustion engines, necessitating the development of newer and better molecules that can be derived from renewable sources.[3−5] Five-carbon alcohols have better fuel properties for internal combustion engines than ethanol as they have a higher blending limit with gasoline, are less hygroscopic, and have a higher energy density.

Two main pathways for five-carbon alcohol production have received considerable attention in the past, namely the mevalonate pathway to isoprenol (Supporting Information, Sup. Figure 1A),[6−8] and the leucine pathway to isopentanol (Sup. Figure 1C).[9] The mevalonate pathway requires three adenosine triphosphate (ATP), three acetyl-CoA, and two NAD(P)H molecules to make isopentenyl pyrophosphate (IPP). The pyrophosphate is then removed by two successive phosphatases yielding isoprenol. Recently a variant of this pathway has been developed that saves one ATP per isoprenol produced (Sup. Figure 1B).[10] The pathway uses a mutated mevalonate pyrophosphate decarboxylase to accept mevalonate phosphate instead of mevalonate pyrophosphate. Thus, one ATP is used to make mevalonate phosphate, and one ATP is used to decarboxylate that intermediate to isopentenyl phosphate. The isopentenyl phosphate can then be dephosphorylated to isoprenol.

Another route to a branched five-carbon alcohol is through leucine biosynthesis to isopentanol (Sup. Figure 1C).[11] The pathway starts with two pyruvates making 2-acetolactate via a decarboxylation. After several steps, including a condensation with acetyl-CoA, the pathway yields 4-methyl-2-oxopentanoate, the direct precursor of leucine. Decarboxylation of 4-methyl-2-oxopentanoate makes 3-methylbutanal, which can then be reduced to 3-methylbutanol, more commonly known as isopentanol. This eight-step pathway uses no ATP, but does require the oxygen sensitive IlvD enzyme.[12]

At first glance the leucine pathway appears more efficient from an ATP standpoint and equal from a carbon standpoint compared to the mevalonate route. However, pairing the mevalonate based pathway with nonoxidative glycolysis[13] makes the combination more carbon efficient than the leucine pathway (Table 1). Nonoxidative glycolysis converts glucose into three acetyl-phosphates which can then be converted to three acetyl-CoAs without any CO_2 loss, and has been demonstrated *in vitro* and *in vivo*.[14,15] Because the mevalonate pathway uses acetyl-CoA exclusively, it is possible to use

Received: October 1, 2019

Table 1. The upper portion of the table shows the stoichiometry of different pathways to C5 alcohols from glucose using only glycolysis. The lower portion of the table shows the stoichiometry of different pathways to make C5 alcohols from glucose balancing glycolysis and nonoxidative glycolysis (NOG) to make the complete pathway as redox balanced as theoretically possible. The mevalonate pathway is abbreviated as MEV.

glycolysis before	input	output	net ATP per glucose	redox balanced
isovaleryl-CoA pathway	3 glucose	2 isopentanol + 6 ATP + 6 Nad(P)H + 8 CO_2	2	no
MEV pathway	3 glucose	2 isoprenol + 0 ATP + 8 Nad(P)H + 8 CO_2	0	no
MEV bypass pathway	3 glucose	2 isoprenol + 2 ATP + 8 Nad(P)H + 8 CO_2	2/3	no
leucine pathway	3 glucose	2 isopentanol + 6 ATP + 6 Nad(P)H + 8 CO_2	2	no
glycolysis balanced with NOG before	**input**	**output**	**net ATP per glucose**	**redox balanced**
isovaleryl-CoA pathway	5 glucose	4 isopentanol + 6 ATP + 10 CO_2 + 6 H_2O	6/5	yes
MEV pathway	7 glucose	6 isoprenol − 12 ATP + 12 CO_2 + 12 H_2O	− 12/7	yes
MEV bypass pathway	7 glucose	6 isoprenol − 6 ATP + 12 CO_2 + 12 H_2O	− 6/7	yes
leucine pathway	4 glucose	3 isopentanol + 6 ATP + 9 CO_2 + 3 Nad(P)H + 3 H_2O	3/2	no

nonoxidative glycolysis to redox balance isoprenol production. The leucine pathway on the other hand cannot be redox balanced from glucose using nonoxidative glycolysis because it requires two pyruvate and one acetyl-CoA (Table 1). Even when the acetyl-CoA is produced via nonoxidative glycolysis the production of each isopentanol yields an extra reducing equivalent.

As biofuels and commodity chemicals have low margins, an optimal pathway for five carbon alcohols would combine the benefits of the leucine pathway and the mevalonate pathway. Mainly a pathway that is both ATP positive and redox balanced thus enabling microaerobic or anaerobic growth conditions. Here we demonstrate a pathway that can produce isopentanol based on the *Myxococcus xanthus* pathway to isovaleryl-CoA.

M. xanthus has previously been noted to produce isovaleryl-CoA for fatty acid biosynthesis in an unusual way.[16] It uses the first two steps of the mevalonate pathway to make HMG-CoA, and then uses a dehydratase to make 3-methylglutaconyl-CoA (Figure 1). This is then decarboxylated to make 3-methylbutenoyl-CoA which can be reduced to isovaleryl-CoA, a fatty acid biosynthesis starter unit. In our work here, we couple this pathway to a butyryl-CoA reductase from *Clostridium acetobutylicum* to make isopentanol.

MODELING

To confirm the thermodynamic viability of the pathway we used the modeling software eQuilibrator.[17] We modeled the worst-case scenario for which the thiolase and HMG-CoA synthase do not have substrate channeling as is possible in certain configurations.[18] The modeling shows the pathway to be thermodynamically feasible, with glycolysis having the lowest min-max driving force (MDF) section of the pathway, and therefore expected to be limiting from a thermodynamic perspective (Figure 2).

EXPERIMENTAL RESULTS

Given the promising modeling results, we constructed several plasmids to test the pathway's viability *in vivo*. We used the p15A origin, chloramphenicol resistance marker, *lacI* and IPTG-inducible P_{LacUV5}-driven operon containing the native sequence of the *Escherichia coli* thiolase *atoB* and the native sequence of *Staphylococcus aureus* HMGS from the plasmid MevTsa-T1002-Ptrc-MKco-PMKco (JPUB_006224) for the expression of the upper portion of the pathway.[7] We based our designs off this plasmid because it showed high IPP flux previously, and the first two genes are common to our pathway. P_{Trc} drives the lower portion of the pathway containing *adhE2* from *Clostridium acetobutylicum*[19] as the isovaleryl-CoA reductive thioesterase (native substrate butyryl-CoA), followed by *aibC*, which encodes the 3-methyl-2-

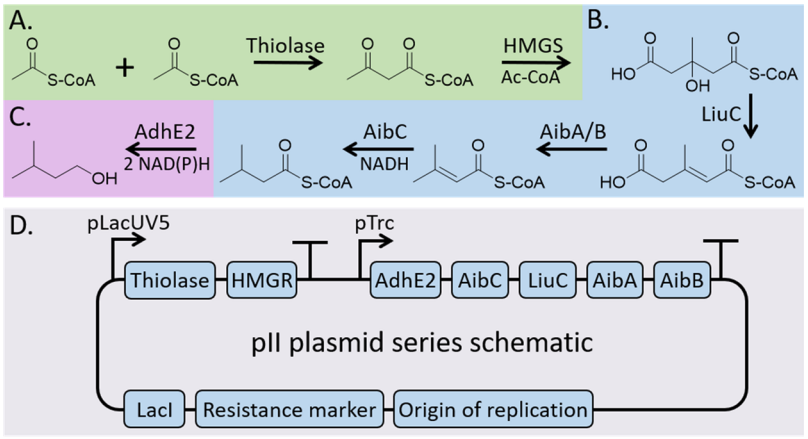

Figure 1. Overview of the isovaleryl-CoA pathway to isopentanol. (A) First two steps of the mevalonate pathway. (B) Isovaleryl-CoA biosynthesis pathway. (C) Final reaction to produce isopentanol requiring an enzyme to catalyze a non-native reaction. (D) Plasmid map schematic for plasmids pII3,5,6,7,8,15. Enzyme abbreviations/natural activity: [HMGS, 3-hydroxy-3-methylglutaryl-coenzyme A synthase]; [LiuC, 3-hydroxy-3-methylglutaryl-coenzyme A dehydratase]; [AibA/B, 3-methylglutaconyl-coenzyme decarboxylase]; [AibC, 3-methylbutenoyl-coenzyme A reductase]; [AdhE2, butyryl-coenzyme A reductase].

https://dx.doi.org/10.1021/acssynbio.9b00402
ACS Synth. Biol. XXXX, XXX, XXX−XXX

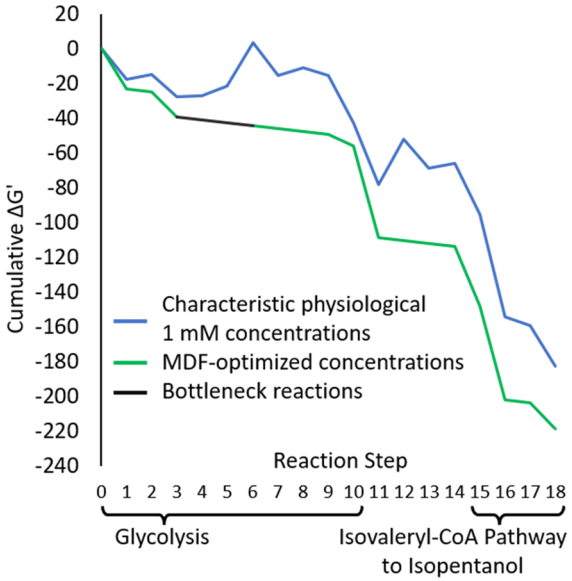

Figure 2. Thermodynamic modeling of the isopentanol production via the isovaleryl-CoA pathway. Metabolites were allowed to vary from 1 μM to 10 mM at pH 7.0 and ionic strength at 0.1 M for the MDF-optimization (default conditions). The predicted bottleneck reactions from a thermodynamic perspective are in glycolysis between the fructose diphosphate aldolase to glyceraldehyde phosphate dehydrogenase reactions.

butenyl-CoA reductase,[16] followed by *liuC* from *Pseudomonas putida*,[20] which encodes the 3-methylglutaconyl-CoA dehydratase, followed by the genes encoding the two halves of the heterodimer 3-methylglutaconyl-CoA decarboxylase, *aibA* and *aibB*.[16] Except when noted above, the amino acid sequences were derived from *Myxococcus xanthus*. All the genes in the P_{Trc}-driven operon were codon optimized for *E. coli* expression with BOOST (https://boost.jgi.doe.gov/).[21] We named this plasmid pII3.

We transformed pII3 into *E. coli* DH1,[22] and expressed the genes as previously reported for C5 alcohol production with minor modifications.[10] pII3 only made trace isopentanol, but made prenol instead at 56.73 ± 5.45 mg/L 24 h after induction in aerobic conditions, and 11.3 ± 2.64 mg/L in microaerobic conditions (Figure 3). We hypothesized that AibC was not expressed at a high enough level to make significant amounts of isovaleryl-CoA and thus isopentanol. To troubleshoot we replaced the *M. xanthus* gene with several different *aibC* homologues codon optimized to express in *E. coli* behind a new RBS predicted to be stronger by the RBS calculator.[23] The *aibC* homologues in pII5 through pII7 are from *Cystobacter fuscus*, *Myxococcus fulvus*, and *Myxococcus stipitatus*, respectively. These genes were found using BLAST[24] and selected for testing based on their relatively high amino acid sequence identity with AibC from *M. xanthus* indicating they likely catalyze the desired reaction. *aibC* in pII8 is an alternately codon optimized gene from *M. xanthus* as compared to pII3. Several of these new plasmids were able to produce isopentanol. pII5 produced the most isopentanol at 10.88 ± 1.15 mg/L 24 h after induction aerobically (Figure 3A) but also produced significant prenol at 24.07 ± 2.26 mg/L as well (Figure 3B). Microaerobic prenol production for pII5 was greatly reduced to 3.46 ± 0.3 mg/L while isopentanol production was increased to 17.59 ± 0.3 mg/L for a selectivity of approximately 5 to 1 isopentanol to prenol (Figure 3).

On the basis of these results we designed a plasmid to increase isopentanol titers and named it pII15. We replaced the origin of replication and resistance marker of pII5 with a high copy number origin of replication, ColE1, and an Amp^R resistance marker from plasmid pJH20 (JPUB_011968).[26] Using the same production and analysis pipeline as before, pII15 produced 20.44 ± 1.82 mg/L isopentanol and 56.26 ± 12.41 mg/L prenol aerobically. The microaerobic condition produced 37.44 ± 4.73 mg/L isopentanol and only 0.66 ± 0.57 mg/L prenol (Figure 3A,B).

Next, we tried another *E. coli* strain XX03 to improve production in microaerobic conditions. XX03 is a BW25113 derivative with knockouts in lactic acid, ethanol, and succinate fermentation genes (*adhE*Δ *ldhA*Δ *frdBC*Δ) to reduce unwanted byproduct formation under microaerobic and anaerobic conditions. We found the pII15 XX03 combination further bolstered isopentanol production to 63.95 ± 2.26 mg/L while maintaining low prenol production, 1.07 ± 0.23 mg/L (Figure 3C).

Finally, with this best strain and plasmid combination we added an oleyl alcohol overlay and took a time course over 36 h, measuring isopentanol, OD_{600}, glucose, and organic acids production (Figure 4). At the 36 h time point the cells had produced 80.50 ± 8.08 mg/L isopentanol, while prenol

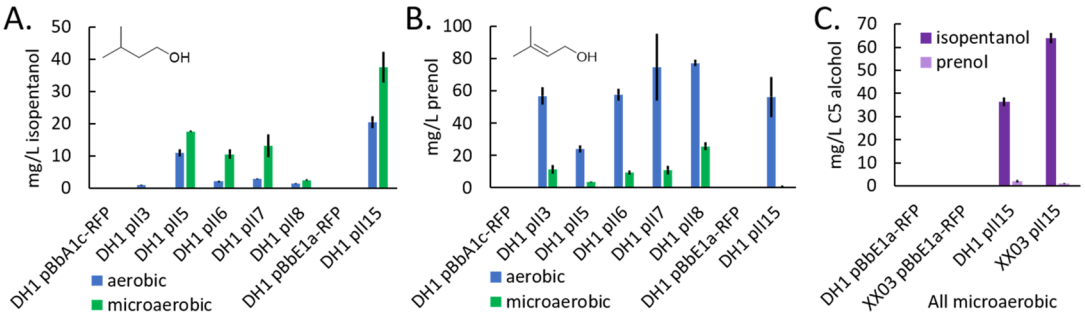

Figure 3. C5 alcohol production 24 h after induction. Plasmids were tested in either *E. coli* DH1 cell line or XX03 (BW25113 *adhE*Δ *ldhA*Δ *frdBC*Δ) in aerobic (200 rpm shaking), or microaerobic (no shaking) conditions in EZ-rich media. pBbA1c-RFP and pBbE1a-RFP are negative control plasmids which express RFP.[25] Error bars represent standard deviation of biological triplicates except for DH1 pII15 and XX03 pII15 in panel C which represent eight biological replicates. (A) Isopentanol production in DH1. (B) Prenol production coproduced from the same cell cultures as in panel A. (C) Microaerobic production of isopentanol and prenol in *E. coli* strains DH1 and XX03. The *aibC* gene origin in the different plasmids are as follows: pII3 *M. xanthus*, pII5 *Cystobacter fuscus*, pII6 *Myxococcus fulvus*, pII7 *Myxococcus stipitatus*, pII8 *M. xanthus* alternate codon optimization, pII15 *Cystobacter fuscus*.

https://dx.doi.org/10.1021/acssynbio.9b00402
ACS Synth. Biol. XXXX, XXX, XXX−XXX

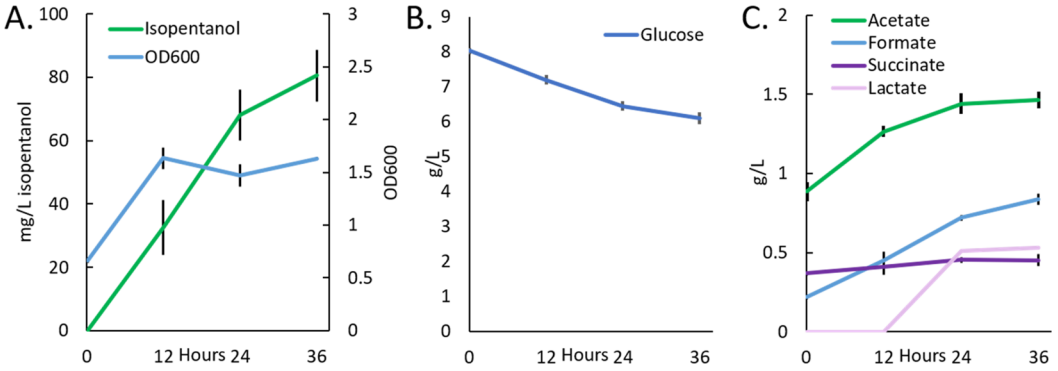

Figure 4. (A) Time course of microaerobic isopentanol production of *E. coli* XX03 with pII15 plasmid with oleyl alcohol overlay in EZ-rich media. Time point zero is when cells were induced. (B) Glucose consumption from the same cultures. (C) Organic acid production from the same cultures. Error bars represent standard deviation of biological triplicate.

production was below the limit of quantification. The cells also produced a significant amount of acetate, up to 1.46 ± 0.05 g/L. The cells did not fully consume the glucose over this time, meaning that significant improvements can still be made to the system.

DISCUSSION

In this work we demonstrated a new isopentanol production pathway inspired by the isovaleryl-CoA pathway from *Myxococcus xanthus*. The pathway requires no ATP and uses the central carbon metabolite acetyl-CoA for C5 alcohol production. A similar pathway was published recently that exclusively makes prenol for incorporation into DMAPP for higher isoprenoid production but was not demonstrated to make isopentanol.[27] Our best construct and strain combination, pII15 and XX03, had a 59-fold preference for isopentanol production over the side product prenol in microaerobic conditions (without the oleyl alcohol overlay). The preference for isopentanol over prenol in microaerobic conditions may be related to the NadH/Nad+ balance of the cell. In aerobic conditions, the cell can regenerate NadH into Nad+ using oxygen, via the electron transport chain. In microaerobic and anaerobic conditions, the cell has a harder time regenerating Nad+, resulting in a higher NadH to Nad+ balance. It is possible this change in redox potential of the cell drives production of isopentanol over prenol in microaerobic conditions.[28]

When designing the pathway, two enzyme types were available for the 3-HMG-CoA dehydratases (LiuC) step.[20] The *Myxococcus xanthus* LiuC can hydrate the pathway intermediate 3-methylbutenoyl-CoA to 3-methyl-3-hydroxybutyryl-CoA, a nonproductive side product.[16] LiuC from *Pseudomonas putida* uses a different reaction mechanism which cannot hydrate 3-methylbutenoyl-CoA and thus avoids a nonproductive side product. However, 3-methylbutenoyl-CoA acts as a competitive inhibitor of this LiuC. We used the LiuC from *Pseudomonas putida* in the current work because reduction of 3-methylbutenoyl-CoA to isovaleryl-CoA is very exothermic. When the pathway is fully optimized hopefully this property will keep 3-methylbutenoyl-CoA levels very low. Empirical testing will be needed to validate this design choice fully.

Because the isovaleryl-CoA to isopentanol pathway derives carbon from acetyl-CoA, it can be coupled to nonoxidative glycolysis. In theory by splitting flux between nonoxidative glycolysis to generate acetyl-CoA, and glycolysis to generate acetyl-CoA, ATP, and NADH, it is possible to produce isopentanol in an ATP positive and redox balanced manner with this pathway. ATP positive and redox balanced pathways can support anaerobic growth as found in the naturally occurring ethanol, lactic acid, and mixed acid fermentation pathways. With the right genomic background lacking alternate fermentation pathways, it would be possible to leverage growth coupling and adaptive laboratory evolution to quickly improve the pathway titer, rate, yield, and tolerance.[29] Thus we believe this pathway is a good choice for further optimization.

MATERIALS AND METHODS

Chemicals. Carbenicillin disodium salt, EZ-rich medium, and LB antibiotic plates were ordered from Teknova. Chloramphenicol was ordered from MP Biomedicals, Inc. Restriction enzyme BsaI, DpnI, T4 DNA ligase, isopropyl *β*-D-1-thiogalactopyranoside (IPTG), and ElectroMAX DH10B cells were ordered from Thermo Fisher Scientific. Molecular grade bovine serum albumin (BSA) was obtained from New England BioLabs. Dextrose (anhydrous) and ethyl acetate were purchased from VWR International. Isoprenol (3-methylbut-3-en-1-ol) was ordered from Acros Organics. Stellar chemically competent cells were purchased from Takara Bio USA. LB (Lennox) and TB powder by Merck KGaA, as well as all other chemicals, were ordered from Sigma-Aldrich.

***In Silico* Modeling.** Min-max driving force (MDF) modeling was conducted with the eQuilibrator[17] web interface (http://equilibrator.weizmann.ac.il/pathway/) using the default parameters for all fields (minimum substrate concentration = 0.001 mM, maximum substrate concentration 10 mM, pH 7.0, ionic strength 0.1 M). We modeled the conversion of three glucose to two five-carbon alcohols (and resulting NADH, ATP, H_2O, and CO_2 production). Modeling files are included in the Supporting Information.

DNA Construction and Sequencing. Primers were designed with DeviceEditor,[30] and Golden Gate assembly[31] was used for assembly. Genes were synthesized by Twist or IDT. Touchdown PCR[32] was used to amplify DNA parts using iProof DNA polymerase. The PCR reaction cycle consisted of 98 °C for 30 s, followed by 10 cycles of 98 °C for 10 s, annealing temperature for 15 s, then extension at 72 °C for 22.5 s per kb of DNA. In the first 10 cycles the annealing temperature was reduced by 0.5 °C each round. After the first 10 cycles, the basic cycle was repeated for another 25 rounds but with no further reduction in annealing temperature. A final extension time of 5 min was added to the end of the program,

https://dx.doi.org/10.1021/acssynbio.9b00402
ACS Synth. Biol. XXXX, XXX, XXX−XXX

before the temperature was reduced to 10 °C until the DNA was used. DNA was then gel purified from a 0.5% agarose gel using QIAquick Gel Extraction Kit before further DNA concentrating with a DNA Clean & Concentrator Kit from Zymo Research. Salts were then removed via dialysis for 30 min using 0.025 μm VWSP membrane filters from Millipore. For assemblies, pieces were mixed in equimolar amounts with a final DNA concentration of the backbone around 33 ng per 5 μL of reaction volume. For Golden Gate assemblies the reaction cycle was used as follows: 25 cycles of 45 °C for 2 min, followed by 5 min of 16 °C, 1 step of 50 °C for 5 min, 1 step of 80 °C for 5 min and then storage at 10 °C until use. Assembled plasmids were transformed into Stellar chemically competent cells, or ElectroMax DH10B cells using the manufacturer's instructions. Plasmids were sequenced essentially as previously published[33,34] using the DIVA seq pipeline. Plasmid maps are available at https://public-registry.jbei.org/folders/434.

DNA Transformation and Cell Culturing. *E. coli* DH1 was transformed using the KCM method. On day one cells were picked from colonies or glycerol stock into Lysogeny Broth (LB) medium and allowed to grow overnight shaking at 200 rpm at 37 °C. On day two cells were back diluted 1:100 into 50 mL of fresh LB and allowed to grow as previously until OD_{600} 0.4. Cells were then chilled on ice for 20 min before centrifuging them at 8000 RCF for 8 min. Supernatant was removed and cells were resuspended in 5 mL of 4 °C TSS (recipe below). Samples of 100 μL of cells were aliquoted into 0.6 mL Eppendorf tubes and either used immediately or flash frozen with liquid nitrogen and stored at −80 °C until future use.

For DNA transformation 1 μL of DNA was added to 100 μL of cells, and 100 μL of 2× KCM (60 mM KCl, 200 mM $CaCl_2$, 100 mM $MgCl_2$) was added. Cells were incubated on ice for approximately 20 min, before being heat shocked for 90 s at 42 °C in a water bath. 200 μL of Terrific Broth (TB) was added and the cells were allowed to recover, without shaking, at 37 °C for an hour before being plated onto plates of the correct antibiotic. When appropriate, carbenicillin was added at a final concentration of 100 μg/mL, and chloramphenicol 30 μg/mL.

To prepare 100 mL TSS, 10 g of polyethylene glycol (molecular weight 3350), 5 mL of dimethyl sulfoxide (DMSO), 2 mL of 1 M $MgCl_2$, were mixed, and LB was added to 100 mL. The mixture was sterile filtered and stored at 4 °C.

Optical density (OD) measurements were taken with a Beckman Coulter DU 800 spectrophotometer at 600 nm.

Five-Carbon Alcohol Fermentation Conditions. The five-carbon alcohol fermentation conditions were as in a previous work.[10] On day one 10 mL of overnight seed cultures were grown in LB at 37 °C shaking at 200 rpm. On day two the overnights were diluted 1 to 100 into 10 mL of EZ-rich medium with 1% glucose, and allowed to grow as before until they reached an OD_{600} between 0.6 and 0.8. Cells were then induced with a final concentration of 1 mM IPTG, and the temperature was reduced to 30 °C at 200 rpm for aerobic conditions of 0 rpm for microaerobic conditions. For conditions with oleyl alcohol overlay, 1 mL of oleyl alcohol was added at the time of IPTG induction. All media contained the appropriate antibiotic.

Five-Carbon Alcohol Extraction. Five-carbon alcohol extraction was conducted essentially as elsewhere.[10] Briefly, 1-butanol was added to a final concentration of 30 mg/L as internal standard in ethyl acetate. Then, 750 μL of cell culture and 750 μL of the ethyl acetate with 1-butanol were vortexed in microcentrifuge tubes for 15 min at max speed. Tubes were then centrifuged in an Eppendorf centrifuge 5424 at max speed (approximately 21100 RCF) for two minutes. A 500 μL aliquot of the upper, nonpolar, ethyl acetate layer was then collected in an amber glass GC vial for analysis.

Five-Carbon Alcohol Extraction of Microaerobic Cultures with Oleyl Alcohol Overlay. Microaerobic cultures with oleyl alcohol were vortexed immediately prior to sampling. A 1.8 mL alliquot of oleyl alcohol and cell culture mixture were collected at 0 h (when IPTG was added for induction), 12, 24, and 36 h. The 1.8 mL cell culture/oleyl alcohol mixture was centrifuged at max speed for two minutes. Then, 250 μL of the supernatant was diluted into 250 μL of ethyl acetate (reduces the viscosity for GC-FID injection) with 1-butanol as internal standard as before. Only one sample was taken from each tube so that tubes were not vortexed multiple times through the microaerobic fermentation.

Analytical Method for Five-Carbon Alcohol Analysis. The analysis of five carbon alcohols was performed essentially as reported elsewhere[8] on a Thermo Scientific Focus GC-FID with a DB-WAX column (15 m long, 0.32 mm diameter, 0.25 μm film thickness). The carrier pressure was set to a constant at 300 kPa, and the inlet temperature was 200 °C. The oven temperature was initially set to 40 °C for 90 s, and then increased at 15 °C a minute until 110 °C. For samples with oleyl alcohol, the final temperature was 250 °C which was held for 3 min. Injection volume was one microliter.

Glucose and Fermentation Products Analysis. For analysis of glucose, acetate, formate, succinate, and lactate, 900 μL of cell culture was centrifuged in an Eppendorf centrifuge 5424 at max speed (approximately 21100 RCF) for 1 min. A 200 μL sample of clarified supernatant was then filtered through AcroPrep 96 well Omega 10K MWCO filter plates at 1500 RCF on an Eppendorf 5810 R centrifuge for 15 min.

Samples were analyzed by isocratic elution with 4 mM sulfuric acid using an HPLC system equipped with an Aminex HPX-87H column (Bio-Rad, Richmond, CA, USA) and a refractive index detector (Agilent Technologies). The flow rate was maintained at 0.6 mL/min, the sample tray was set to 4 °C, and the column compartment temperature was set to 50 °C. Data acquisition and analysis were performed via Chemstation software (Agilent Technologies).

Data Availability. Plasmid maps are available in the JBEI public registry (https://public-registry.jbei.org/folders/434).[35] Supplemental data is available at the Experiment Data Depot (EDD) (https://public-edd.jbei.org/s/eiben-et-al-c5-alcohol-production/overview/).[36] See the Supporting Information data file for additional information about strain names for archive requests from corresponding author, Addgene, or Molecular Cloud.

■ ASSOCIATED CONTENT

Supporting Information

The Supporting Information is available free of charge at https://pubs.acs.org/doi/10.1021/acssynbio.9b00402.

Sup. Figure 1; Sup. Figure 2 (PDF)

Data set_S1 table of contents. Data set_S1: Contains DH1_C5_AlcoholData, eQuilibratorModeling, SupplementalTable1, SupplementalTable2, SupplementalTable3, and SupplementalTable4 (XLSX)

https://dx.doi.org/10.1021/acssynbio.9b00402
ACS Synth. Biol. XXXX, XXX, XXX−XXX

AUTHOR INFORMATION

Corresponding Author

Jay D. Keasling − *Department of Bioengineering, Department of Chemical & Biomolecular Engineering, and Institute for Quantitative Biosciences, University of California, Berkeley, Berkeley, California 94270, United States; Joint BioEnergy Institute, Emeryville, California 94608, United States; Biological Systems & Engineering Division, Lawrence Berkeley National Laboratory, Berkeley, California 94720, United States; Novo Nordisk Foundation Center for Biosustainability, Technical University of Denmark, Kogle Alle, Hørsholm DK2970, Denmark; Center for Synthetic Biochemistry, Institute for Synthetic Biology, Shenzhen Institutes for Advanced Technologies, Shenzhen 518055, China;* orcid.org/0000-0003-4170-6088

Authors

Christopher B. Eiben − *Department of Bioengineering, University of California, Berkeley, Berkeley, California 94270, United States; Department of Bioengineering, University of California, San Francisco, California 94143, United States*

Tian Tian − *Joint BioEnergy Institute, Emeryville, California 94608, United States; Biological Systems & Engineering Division, Lawrence Berkeley National Laboratory, Berkeley, California 94720, United States*

Mitchell G. Thompson − *Joint BioEnergy Institute, Emeryville, California 94608, United States; Biological Systems & Engineering Division, Lawrence Berkeley National Laboratory, Berkeley, California 94720, United States; Department of Plant and Microbial Biology, University of California, Berkeley, Berkeley, California 94270, United States*

Daniel Mendez-Perez − *Joint BioEnergy Institute, Emeryville, California 94608, United States; Biological Systems & Engineering Division, Lawrence Berkeley National Laboratory, Berkeley, California 94720, United States*

Nurgul Kaplan − *Joint BioEnergy Institute, Emeryville, California 94608, United States; Biological Systems & Engineering Division, Lawrence Berkeley National Laboratory, Berkeley, California 94720, United States; Agile BioFoundry, Emeryville, California 94608, United States*

Garima Goyal − *Joint BioEnergy Institute, Emeryville, California 94608, United States; Biological Systems & Engineering Division, Lawrence Berkeley National Laboratory, Berkeley, California 94720, United States; Agile BioFoundry, Emeryville, California 94608, United States*

Jennifer Chiniquy − *Joint BioEnergy Institute, Emeryville, California 94608, United States; Biological Systems & Engineering Division, Lawrence Berkeley National Laboratory, Berkeley, California 94720, United States; Agile BioFoundry, Emeryville, California 94608, United States*

Nathan J. Hillson − *Joint BioEnergy Institute, Emeryville, California 94608, United States; Biological Systems & Engineering Division, Lawrence Berkeley National Laboratory, Berkeley, California 94720, United States; Agile BioFoundry, Emeryville, California 94608, United States;* orcid.org/0000-0002-9169-3978

Taek Soon Lee − *Joint BioEnergy Institute, Emeryville, California 94608, United States; Biological Systems & Engineering Division, Lawrence Berkeley National Laboratory, Berkeley, California 94720, United States;* orcid.org/0000-0002-0764-2626

Complete contact information is available at: https://pubs.acs.org/10.1021/acssynbio.9b00402

Author Contributions

C.B.E. conceived the project, designed and cloned plasmids, helped design the experiments and wrote the manuscript. T.T. designed and cloned plasmids and designed and performed experiments. M.G.T. and D.M.P. helped with data acquisition and analysis. N.K. and G.G. performed PCRs for plasmid construction. J.C. deep sequenced plasmids. N.J.H. edited and contributed to insights in the manuscript and oversaw plasmid construction efforts. T.S.L. oversaw T.T. and experiments. J.D.K. helped write the manuscript and provided project guidance.

Funding

C.B.E. was supported by National Science Foundation (NSF) Graduate Research Fellowship Program (DGE-1106400) and National Institute of Health training Grant T32 GM008295. NSF Grant 0540879 supported the materials for this work. This work was part of the DOE Joint BioEnergy Institute (https://www.jbei.org) supported by the U.S. Department of Energy, Office of Science, Office of Biological and Environmental Research, and was part of the Agile BioFoundry (https://agilebiofoundry.org) supported by the U.S. Department of Energy, Energy Efficiency and Renewable Energy, Bioenergy Technologies Office, through contract DE-AC02-05CH11231 between Lawrence Berkeley National Laboratory and the U.S. Department of Energy. The views and opinions of the authors expressed herein do not necessarily state or reflect those of the United States Government or any agency thereof. Neither the United States Government nor any agency thereof, nor any of their employees, makes any warranty, expressed or implied, or assumes any legal liability or responsibility for the accuracy, completeness, or usefulness of any information, apparatus, product, or process disclosed, or represents that its use would not infringe privately owned rights. The United States Government retains and the publisher, by accepting the article for publication, acknowledges that the United States Government retains a nonexclusive, paid-up, irrevocable, worldwide license to publish or reproduce the published form of this manuscript, or allow others to do so, for United States Government purposes. The Department of Energy will provide public access to these results of federally sponsored research in accordance with the DOE Public Access Plan (http://energy.gov/downloads/doe-public-access-plan).

Notes

The authors declare the following competing financial interest(s): J.D.K. has a financial interest in Amyris, Lygos, Demetrix, Maple Bio, and Napigen. C.B.E. has a financial interest in Perlumi Chemicals.

ACKNOWLEDGMENTS

The authors would like to thank Dr. Xinkai Xie for providing *E. coli* strain XX03.

REFERENCES

(1) Intergovernmental Panel on Climate Change Working Group III, and Edenhofer, O. (2014) *Climate change 2014: Mitigation of climate change: Working Group III contribution to the Fifth Assessment Report of the Intergovernmental Panel on Climate Change*, Cambridge University Press, New York, NY.

(2) Neupane, B., Konda, N. V. S. N. M., Singh, S., Simmons, B. A., and Scown, C. D. (2017) Life-Cycle Greenhouse Gas and Water Intensity of Cellulosic Biofuel Production Using Cholinium Lysinate Ionic Liquid Pretreatment. *ACS Sustainable Chem. Eng. 5*, 10176−10185.

(3) Hansen, A. C., Zhang, Q., and Lyne, P. W. L. (2005) Ethanol-diesel fuel blends – a review. *Bioresour. Technol. 96*, 277−285.
(4) Zargar, A., Bailey, C. B., Haushalter, R. W., Eiben, C. B., Katz, L., and Keasling, J. D. (2017) Leveraging microbial biosynthetic pathways for the generation of "drop-in" biofuels. *Curr. Opin. Biotechnol. 45*, 156−163.
(5) Haushalter, R. W., Kim, W., Chavkin, T. A., The, L., Garber, M. E., Nhan, M., Adams, P. D., Petzold, C. J., Katz, L., and Keasling, J. D. (2014) Production of anteiso-branched fatty acids in Escherichia coli; next generation biofuels with improved cold-flow properties. *Metab. Eng. 26*, 111−118.
(6) George, K. W., Thompson, M. G., Kang, A., Baidoo, E., Wang, G., Chan, L. J. G., Adams, P. D., Petzold, C. J., Keasling, J. D., and Lee, T. S. (2015) Metabolic engineering for the high-yield production of isoprenoid-based C alcohols in E. coli. *Sci. Rep. 5*, 11128.
(7) George, K. W., Chen, A., Jain, A., Batth, T. S., Baidoo, E. E. K., Wang, G., Adams, P. D., Petzold, C. J., Keasling, J. D., and Lee, T. S. (2014) Correlation analysis of targeted proteins and metabolites to assess and engineer microbial isopentenol production. *Biotechnol. Bioeng. 111*, 1648−1658.
(8) Chou, H. H., and Keasling, J. D. (2012) Synthetic pathway for production of five-carbon alcohols from isopentenyl diphosphate. *Appl. Environ. Microbiol. 78*, 7849−7855.
(9) Atsumi, S., Hanai, T., and Liao, J. C. (2008) Non-fermentative pathways for synthesis of branched-chain higher alcohols as biofuels. *Nature 451*, 86−89.
(10) Kang, A., George, K. W., Wang, G., Baidoo, E., Keasling, J. D., and Lee, T. S. (2016) Isopentenyl diphosphate (IPP)-bypass mevalonate pathways for isopentenol production. *Metab. Eng. 34*, 25−35.
(11) Gronenberg, L. S., Marcheschi, R. J., and Liao, J. C. (2013) Next generation biofuel engineering in prokaryotes. *Curr. Opin. Chem. Biol. 17*, 462−471.
(12) Flint, D. H., Emptage, M. H., Finnegan, M. G., Fu, W., and Johnson, M. K. (1993) The role and properties of the iron-sulfur cluster in Escherichia coli dihydroxy-acid dehydratase. *J. Biol. Chem. 268*, 14732−14742.
(13) Bogorad, I. W., Lin, T.-S., and Liao, J. C. (2013) Synthetic non-oxidative glycolysis enables complete carbon conservation. *Nature 502*, 693−697.
(14) Lin, P. P., Jaeger, A. J., Wu, T.-Y., Xu, S. C., Lee, A. S., Gao, F., Chen, P.-W., and Liao, J. C. (2018) Construction and evolution of an Escherichia coli strain relying on nonoxidative glycolysis for sugar catabolism. *Proc. Natl. Acad. Sci. U. S. A. 115*, 3538−3546.
(15) Meadows, A. L., Hawkins, K. M., Tsegaye, Y., Antipov, E., Kim, Y., Raetz, L., Dahl, R. H., Tai, A., Mahatdejkul-Meadows, T., Xu, L., Zhao, L., Dasika, M. S., Murarka, A., Lenihan, J., Eng, D., Leng, J. S., Liu, C.-L., Wenger, J. W., Jiang, H., Chao, L., Tsong, A. E., et al. (2016) Rewriting yeast central carbon metabolism for industrial isoprenoid production. *Nature 537*, 694−697.
(16) Li, Y., Luxenburger, E., and Müller, R. (2013) An alternative isovaleryl CoA biosynthetic pathway involving a previously unknown 3-methylglutaconyl CoA decarboxylase. *Angew. Chem., Int. Ed. 52*, 1304−1308.
(17) Flamholz, A., Noor, E., Bar-Even, A., and Milo, R. (2012) eQuilibrator–the biochemical thermodynamics calculator. *Nucleic Acids Res. 40*, D770−5.
(18) Vögeli, B., Engilberge, S., Girard, E., Riobé, F., Maury, O., Erb, T. J., Shima, S., and Wagner, T. (2018) Archaeal acetoacetyl-CoA thiolase/HMG-CoA synthase complex channels the intermediate via a fused CoA-binding site. *Proc. Natl. Acad. Sci. U. S. A. 115*, 3380−3385.
(19) Bond-Watts, B. B., Bellerose, R. J., and Chang, M. C. Y. (2011) Enzyme mechanism as a kinetic control element for designing synthetic biofuel pathways. *Nat. Chem. Biol. 7*, 222−227.
(20) Wong, B. J., and Gerlt, J. A. (2004) Evolution of function in the crotonase superfamily: (3S)-methylglutaconyl-CoA hydratase from Pseudomonas putida. *Biochemistry 43*, 4646−4654.
(21) Oberortner, E., Cheng, J.-F., Hillson, N. J., and Deutsch, S. (2017) Streamlining the Design-to-Build Transition with Build-Optimization Software Tools. *ACS Synth. Biol. 6*, 485−496.
(22) Peralta-Yahya, P. P., Ouellet, M., Chan, R., Mukhopadhyay, A., Keasling, J. D., and Lee, T. S. (2011) Identification and microbial production of a terpene-based advanced biofuel. *Nat. Commun. 2*, 483.
(23) Salis, H. M. (2011) The ribosome binding site calculator. *Methods Enzymol. 498*, 19−42.
(24) Zhang, Z., Schwartz, S., Wagner, L., and Miller, W. (2000) A greedy algorithm for aligning DNA sequences. *J. Comput. Biol. 7*, 203−214.
(25) Lee, T. S., Krupa, R. A., Zhang, F., Hajimorad, M., Holtz, W. J., Prasad, N., Lee, S. K., and Keasling, J. D. (2011) BglBrick vectors and datasheets: A synthetic biology platform for gene expression. *J. Biol. Eng. 5*, 12.
(26) Eiben, C. B., de Rond, T., Bloszies, C., Gin, J., Chiniquy, J., Baidoo, E. E. K., Petzold, C. J., Hillson, N. J., Fiehn, O., and Keasling, J. D. (2019) Mevalonate pathway promiscuity enables noncanonical terpene production. *ACS Synth. Biol. 8*, 2238−2247.
(27) Clomburg, J. M., Qian, S., Tan, Z., Cheong, S., and Gonzalez, R. (2019) The isoprenoid alcohol pathway, a synthetic route for isoprenoid biosynthesis. *Proc. Natl. Acad. Sci. U. S. A. 116*, 12810−12815.
(28) San, K.-Y., Bennett, G. N., Berríos-Rivera, S. J., Vadali, R. V., Yang, Y.-T., Horton, E., Rudolph, F. B., Sariyar, B., and Blackwood, K. (2002) Metabolic engineering through cofactor manipulation and its effects on metabolic flux redistribution in Escherichia coli. *Metab. Eng. 4*, 182−192.
(29) Portnoy, V. A., Bezdan, D., and Zengler, K. (2011) Adaptive laboratory evolution–harnessing the power of biology for metabolic engineering. *Curr. Opin. Biotechnol. 22*, 590−594.
(30) Chen, J., Densmore, D., Ham, T. S., Keasling, J. D., and Hillson, N. J. (2012) Device Editor visual biological CAD canvas. *J. Biol. Eng. 6*, 1.
(31) Engler, C., Kandzia, R., and Marillonnet, S. (2008) A one pot, one step, precision cloning method with high throughput capability. *PLoS One 3*, No. e3647.
(32) Saiki, R. K., Scharf, S., Faloona, F., Mullis, K. B., Horn, G. T., Erlich, H. A., and Arnheim, N. (1985) Enzymatic amplification of beta-globin genomic sequences and restriction site analysis for diagnosis of sickle cell anemia. *Science 230*, 1350−1354.
(33) Thompson, M. G., Sedaghatian, N., Barajas, J. F., Wehrs, M., Bailey, C. B., Kaplan, N., Hillson, N. J., Mukhopadhyay, A., and Keasling, J. D. (2018) Isolation and characterization of novel mutations in the pSC101 origin that increase copy number. *Sci. Rep. 8*, 1590.
(34) Chiniquy, J., Garber, M. E., Mukhopadhyay, A., and Hillson, N. J. (2020) Fluorescent amplification for next generation sequencing (FA-NGS) library preparation. *BMC Genomics 21*, 85.
(35) Ham, T. S., Dmytriv, Z., Plahar, H., Chen, J., Hillson, N. J., and Keasling, J. D. (2008) Design, implementation and practice of JBEI-ICE: an open source biological part registry platform and tools. *Nucleic Acids Res. 40*, No. e141.
(36) Morrell, W. C., Birkel, G. W., Forrer, M., Lopez, T., Backman, T. W. H., Dussault, M., Petzold, C. J., Baidoo, E. E. K., Costello, Z., Ando, D., Alonso-Gutierrez, J., George, K. W., Mukhopadhyay, A., Vaino, I., Keasling, J. D., Adams, P. D., Hillson, N. J., and Garcia Martin, H. (2017) The Experiment Data Depot: A Web-Based Software Tool for Biological Experimental Data Storage, Sharing, and Visualization. *ACS Synth. Biol. 6*, 2248−2259.

https://dx.doi.org/10.1021/acssynbio.9b00402
ACS Synth. Biol. XXXX, XXX, XXX−XXX